EFFECT OF OPERATIONAL CONDITIONS ON ENERGY EFFICIENCIES OF AIR-SWEPT BALL MILL AND CLASSIFICATION CIRCUITS IN CEMENT RAW MATERIAL PRODUCTION

Ö. Genç [1,*], A.H. Benzer [2]

[1]*Muğla Sıtkı Koçman University, Mining Engineering Department*
*(*Sorumlu yazar: ogenc@mu.edu.tr)*
[2]*Hacettepe University, Mining Engineering Department*

ABSTRACT

Operational performance and energy efficiencies of cement raw material grinding air-swept ball mill and classification circuits were analysed and discussed in this study. Extensive sampling surveys were performed around the circuits A and B in which single compartment air-swept ball mills with dimensions of ∅3.8xL10m and ∅3.8xL10.15m respectively were closed circuited with static air classifiers. Operational results demonstrated that, specific energy savings of 48.47% in ball mill grinding can be achieved with the operational conditions in circuit-B as compared to the conditions in circuit-A. Ball mill with the same dimensions can be operated as much more energy efficient depending mainly on the feed fineness and grindability values. Mill raw material feed particle size distribution fineness and work index values were the important parameters in obtaining finer material from the mill. However, air classifier should also be operated at its optimum operating conditions in obtaining finer final product from the grinding circuit.

In this context, various ways to alter the fineness and grindabilities of raw materials should be investigated so that to increase the capacity rates of air-swept ball milling circuits in raw material production line. For example; application of pre-crushers as High Pressure Grinding Rollers (HPGRs), integration of screens to the circuits, optimization of blasting conditions in the open-pit mining stage and attaining of optimum operational conditions for the air classifier.

Keywords: Grinding, classification, energy, cement raw material

INTRODUCTION

Two types of mills are used widely for the production of raw meal in the industry which are grinding and drying roller mills and ball mills as stated in Ghosh (1991). Ball mills are grate discharge or air-swept types (Duda, 1985; Genç, 2008). Roller mills are frequently used as compared to ball mills due to the lower energy consumption figures of about 10kWh/t as given in Ghosh (1991). Roller mills also have more compact design and thus, smaller in dimension as stated in Genç (2008). Air-swept ball mills usually have pre-drying compartments arranged in front of the grinding compartment of the mill and the pre-drying compartment is equipped with lifters and grinding media is not applied as given in Duda (1985). The pre-drying compartment is separated from the grinding compartment by a partition and flue gases enter and leave the mill through the feed and discharge trunnion (Duda, 1985). There is a bucket elevator in grate discharge mill arrangement for carrying the circulating loads and circulating load is carried pneumatically in air-swept grinding mill arrangement as explained by Duda (1985). The advantage of the air-swept grinding mill is its suitability for utilizing great amounts of waste gases and thus, the energy consumption for an air-swept grinding circuit is higher by approximately 10-12% as compared to the grinding circuit with bucket elevator. Provisions can be made for an adequate amount of hot gases to enter the mill to attain a high grinding efficiency and a by-pass arrangement can be used to control the amount of gases to satisfy operational requirements. Air stream takes the ground product

out of the mill and carries it upwards to a gravity type separator and then to a cyclone where the fines are separated from the gas (Duda, 1985).

Grinding stage consumes the highest energy during the production of raw meal and thus, optimum operational conditions should be maintained to reduce the energy consumption of production. In this respect, performance analysis of the air-swept ball mill and static air classifier circuits in raw meal preparation stage were performed and compared to analyse the energy efficiencies of grinding stage in relation to the operational conditions of the grinding and classification circuit.

EXPERIMENTAL

Description of the Circuits

Extensive sampling studies were conducted around grinding and classification circuits in Plant-A (Circuit-A) and Plant-B (Circuit-B) respectively to analyse the size reduction and classification performances. Design specifications of the ball mills are given in Table 1. Ball size distributions applied in the circuits are given in Table 2. Comparison of the ball size distribution fineness as cumulative passing % are presented in Figure 1.

Table 1. Design specifications of the ball mills

Parameters	Circuit-A	Circuit-B
Mill diameter (m)	3.8	3.8
Mill length (m)	10	10.15
Mill rotational speed (rev/min)	15	16.1
Mill motor power (kW)	1240	1000
Volumetric air flowrate (m^3/h) at 100% fan opening	132700	230100

Table 2. Ball charge distributions in the ball mill

Ball size (mm)	Circuit-A Weight %	Circuit-B Weight %
90	0.00	-
80	3.60	-
70	21.90	13.99
60	23.20	17.48
50	21.20	8.39
40	21.70	13.29
30	8.50	21.68
25	-	25.17
total	100.00	100.00

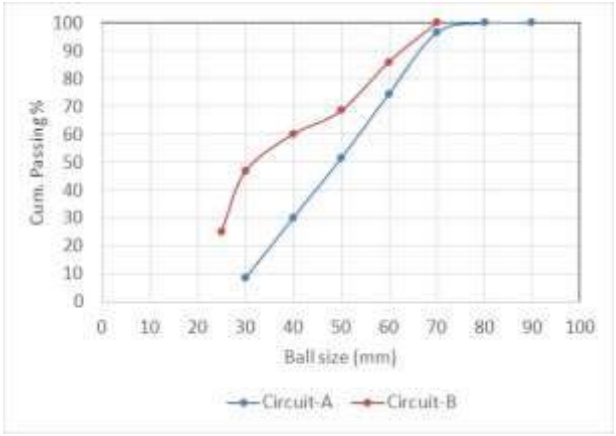

Figure 1. Comparison of the ball size distribution fineness

Sampling Surveys Around the Circuits

Flowsheets of the circuits are given in Figure 2 and 3 with the sampling points. Single compartment ball mills with dimensions of ∅3.8xL10m and ∅3.8xL10.15m were operating in closed circuit with static air classifiers in the sampled circuits. Limestone, clay and iron ore were the raw materials in both circuits. Electrofilter discharge material was added to the static separator fine in circuit-A. Finer ball size distribution was applied in circuit-B as compared to circuit-A depending on the fresh feed particle size distributions.

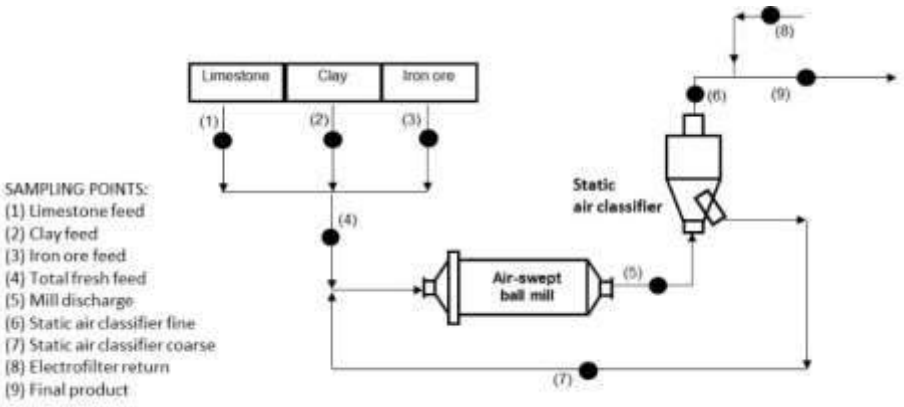

Figure 2. Flowsheet of Circuit-A

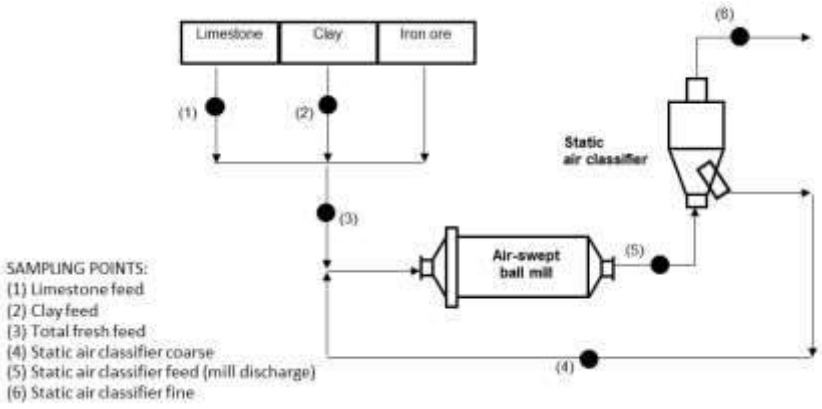

Figure 3. Flowsheet of Circuit-B

Sampling Surveys Inside the Ball Mills

Mills were crash-stopped and cooled down for about 9 hours for inside mill sampling following sampling studies around the circuits. Sampling locations inside the mills are given in Table 3 for the ball mills in circuit-A and circuit-B respectively. Inside mill samples were collected along the long axis of the mills for about each meter. Thus, eleven sampling points were formed by digging out the material for about 40cm below the surface at each meter. Representative amount of samples were collected at each sampling location and are given in Table 3.

Table 3. Sampling locations and sample amounts inside the ball mills in circuit-A and circuit-B

Circuit A	Grinding chamber length (m)	0 (chamber inlet)	1	2	3	4	5	6.7	7.4			
	Condition	-	X	X	X	X	X	X	X	-	-	-
	Sample (kg)		10.42	6.60	7.96	5.79	3.91	3.43	3.83			
Circuit B	Grinding chamber length (m)	0 (chamber inlet)	1	2	3	4	5	6	7	8	9	10
	Condition	X	X	X	X	X	X	X	X	X	X	X
	Sample (kg)	9.51	3.92	3.07	3.52	2.35	2.21	2.79	2.60	1.66	1.90	2.48

X: Sample was collected at the regarded location

RESULTS AND DISCUSSIONS

Material Characterization

Standard Bond Work Index Tests

Standard Bond work index tests were performed by using a 90µm Tyler test sieve according to Bond's procedure as stated in Austin et.al. (1984). Bond work index of the mill feeds were determined as 11.03 kWh/t and 8.58 kWh/t in circuit-A and circuit-B respectively. Bond work index values were observed to change in each survey.

Determination of Particle Size Distributions

Particle size distributions of the samples were determined by dry hand sieving from the top size (75mm) down to 9.5mm. Sub-sieve sample of 9.5mm which is -9.5mm material was sampled for Ro-tap sieving down to 150µm. -150µm material was sampled for the particle size distribution analysis by using the dry mode of the SYMPATHEC® laser diffractometer. Screening and laser diffractometer results were combined mathematically to obtain the full size distribution from the top size down to 1.8µm.

Mass Balancing of the Circuits

Mass balance of the circuits in Plant-A and Plant-B were performed by using JKSimMet Software V4.32. Tonnage flowrates and fineness distributions which were represented by the value of cumulative weight % of 45µm around the circuits are given in Figures 4 and 5. Agreement between the experimental and calculated (mass balanced) particle size distributions are given in Figures 6 and 7 for

Circuit-A and Circuit-B respectively. Satisfactorily good agreement was observed between experimentally measured and calculated values by mass balance calculations. Thus, the data can be used in size reduction and classification performance evaluation.

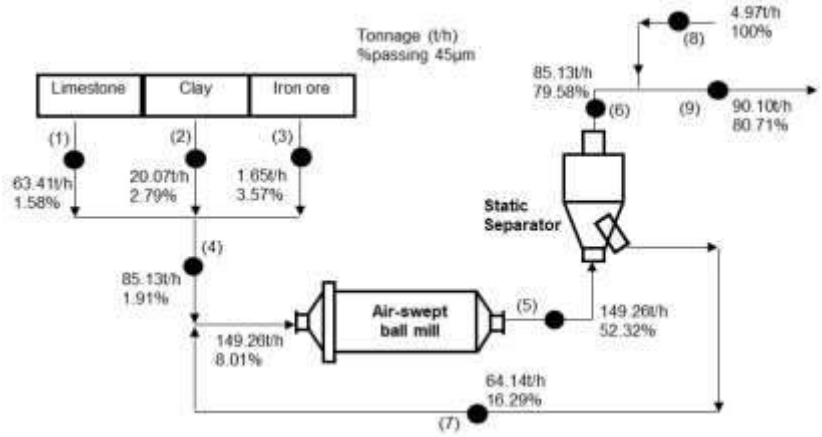

Figure 4. Mass balance results of Circuit-A

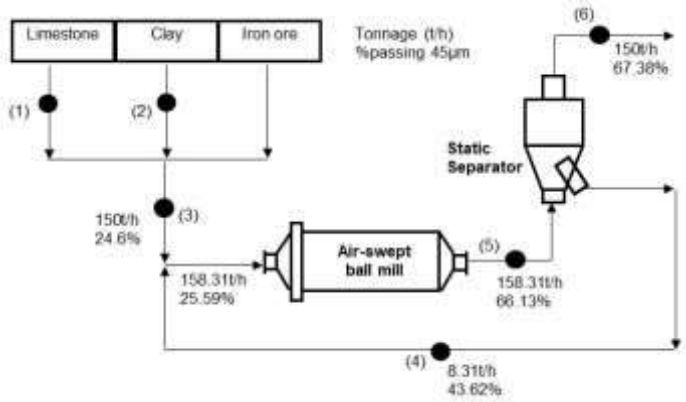

Figure 5. Mass balance results of Circuit-B

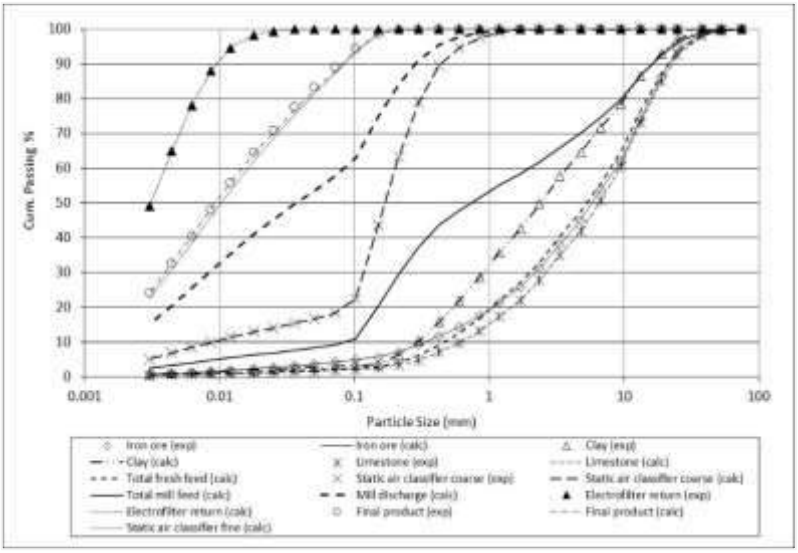

Figure 6. Experimental and mass balanced particle size distributions in Circuit-A

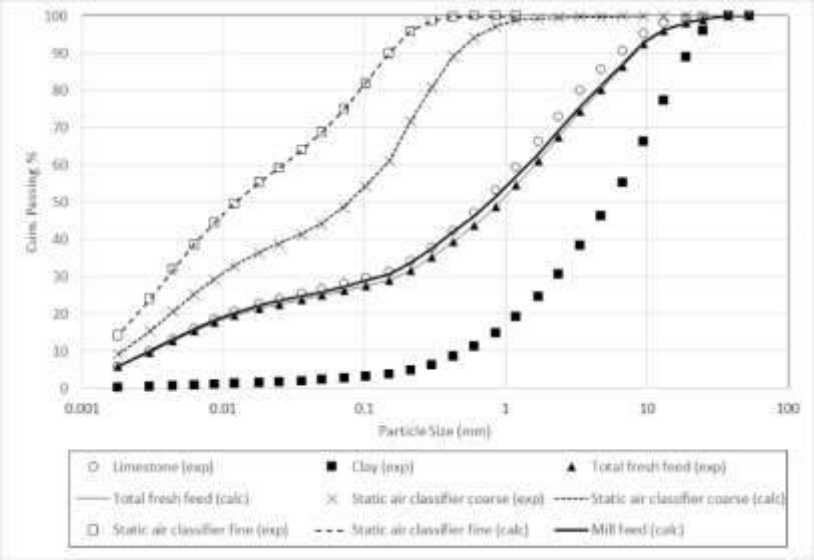

Figure 7. Experimental and mass balanced particle size distributions in Circuit-B

Ball Mill Inside Particle Size Distributions

Ball mill inside particle size distributions are given for circuit-A and circuit-B in Figures 8 and 9 respectively. Calculated mill feed and discharge particle size distributions by mass balancing of the circuits are also given in the regarded Figures.

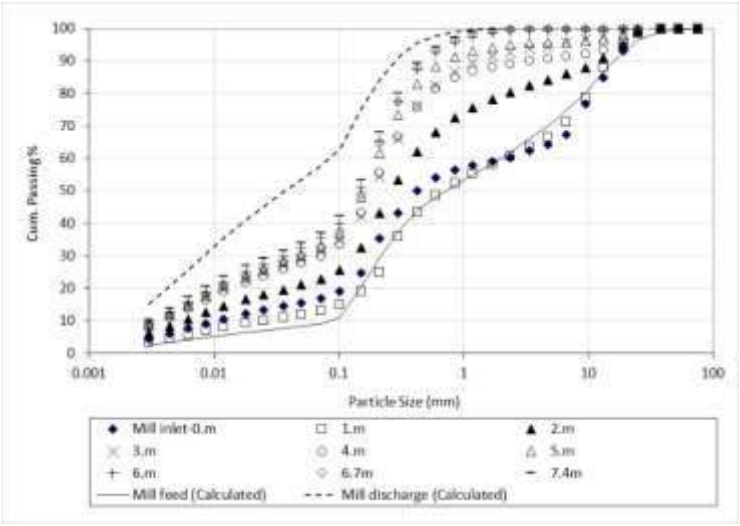

Figure 8. Ball mill inside particle size distributions in circuit-A

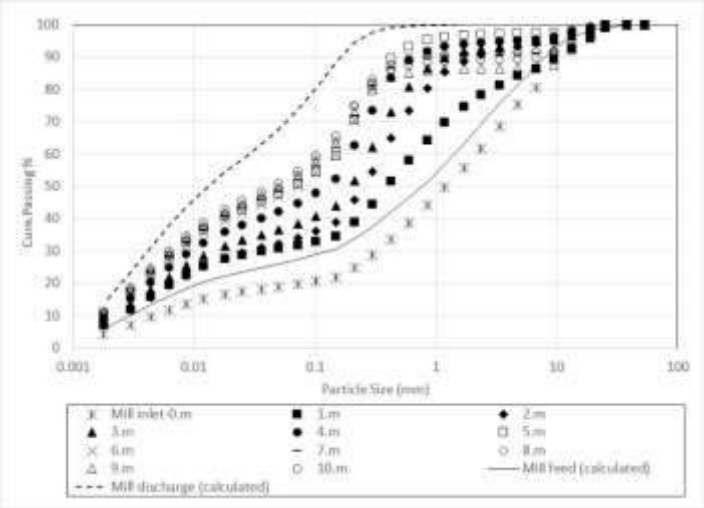

Figure 9. Ball mill inside particle size distributions in circuit-B

Inside mill particle size distributions in circuit-A indicated a relatively consistent size reduction from the first meter towards the third meters of the grinding compartment length. However, particle size distribution got slightly coarser at the fourth meters of the compartment which indicated a decrease in size reduction performance inside the mill. It could be due to internal mill material mixing effect or inside mill ball size classification performance. Particle size distribution got finer again in the fifth meters indicating improvement in size reduction performance. Size reduction progress could have been achieved towards the seven point four meters of the compartment length. Significant change in the particle size distributions of the samples belonging to sixth and six point seven meters of the compartment length as the regarding sampling points were selected to be very close to each other and mixing effect prevailed. Overall size reduction progress thus, performance was found to be consistent. Inside mill particle size distributions in circuit-B indicated a consistent size reduction from the first meter towards the fifth meters of the compartment length. Size reduction performance was observed to decrease at the last five meters of the compartment length. Particle accumulation above about 600μm was observed at the last five meters. Size reduction progress could not have been observed at the last five meters due to the accumulation effect. Measured mill inlet particle size distribution was found to be coarser than the calculated mill feed particle size distribution. This effect could be related to the mixing inside the mill due to the air classifier reject particle size distribution at the crash-stop condition. Thus, particle size distribution of this point was not considered in the size reduction performance evaluation. Overall size reduction progress was determined to be consistent in the first five meters of the compartment length.

Size Reduction Performance Evaluation

Circuit fresh feed particle size distributions are compared in Figure 10. Fresh feed particle size distribution in circuit-B was observed to be more finer than the one in circuit-A. Additionally, more finer mill discharge particle size distribution was obtained in circuit-B which is given in Figure 11. Size reduction ratio was defined for the milling conditions based on X80 and X50 particle sizes of the mill feed and discharge. Relationship is given for X80 particle size in Equation 1.

$$Size\ Reduction\ Ratio = \frac{X80_{mill\ feed}}{X80_{mill\ discharge}} \quad (1)$$

Size reduction ratios based on the X80 and X50 sizes are compared in Table 4. which indicated the grinding performance. Size reduction performance of the mill was determined to be higher in circuit-A as compared to circuit-B based on the X80 size. However, much lower size reduction ratio was

obtained in the fine size ranges which was represented by the X50 size. Thus, size reduction performance was considerably increased in the fine size ranges in finer feed condition. Operational parameters and specific energy consumptions in circuit-A and circuit-B are given in Table 5. Circulating loads were observed to change as 71% and 6% in circuit-A and circuit-B respectively. Circulating load was also decreased at finer fresh feed condition. Much finer particle size distribution was obtained in static air classifier fine stream in circuit-A as given in Figure 12. Ball mill in circuit-B was recorded to be operated about 48.47% energy efficient as compared to the mill in circuit-A under the stated operational conditions in Table 5.

Table 4. Size reduction ratio and circulating load variations

	Circuit-A		**Circuit-B**	
	X80	X50	X80	X50
Mill feed	9.3	0.7	4.2	0.74
Mill discharge	0.18	0.037	0.1	0.013
Size reduction ratio	52	19	42	57

Table 5. Operational parameters and specific energy consumptions in circuit-A and circuit-B

	Circuit-A	**Circuit-B**
Circulating load %	71	6
Air classifier feed rate (t/h)	149.26	158.31
Circuit capacity rate (t/h)	90.10	150
Specific Energy (kWh/t)	13.76	6.67

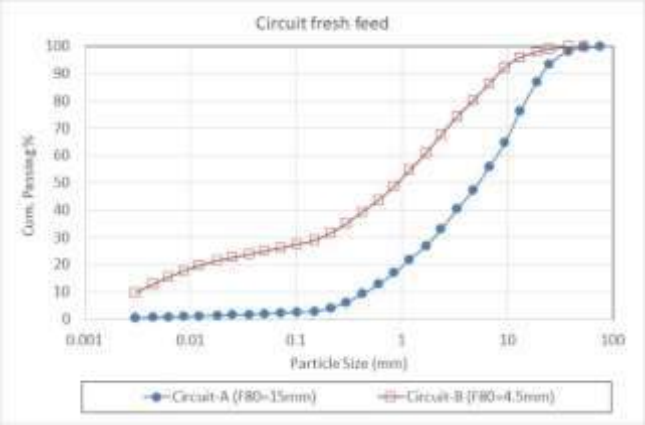

Figure 10. Particle size distributions of circuit fresh feed in circuit-A and circuit-B

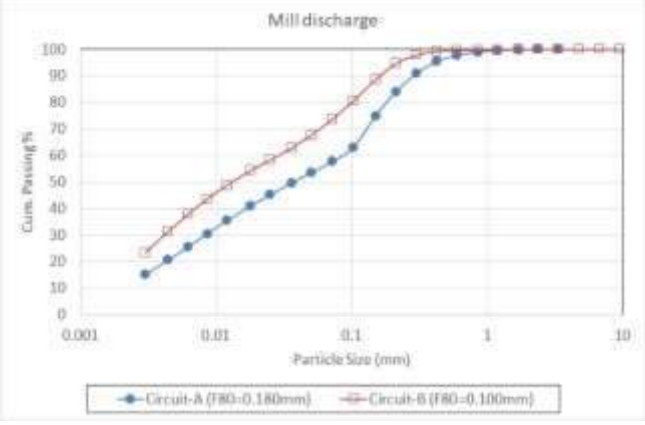

Figure 11. Particle size distributions of mill discharge in circuit-A and circuit-B

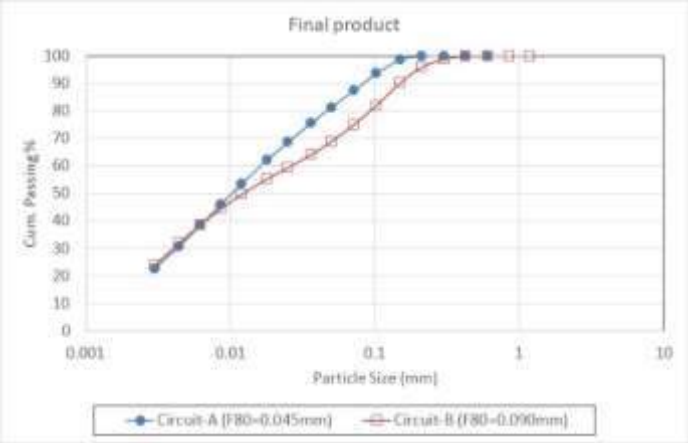

Figure 12. Particle size distributions of final product in circuit-A and circuit-B

Static Air-classifier Performance Evaluation

Classification performance of the static air classifiers in the circuits were evaluated by the partition or efficiency curve approach which describes the proportion of a given size of solids that reports to the underflow or overflow products as given in Napier Munn et.al. (2005). Underflow product corresponds to reject stream and overflow product corresponds to fine stream in air classifiers. Partition coefficients were calculated from Equation 2.

$$Partition\ Coefficient = \frac{Uu}{Ff} \times 100 \quad (2)$$

Where;

U : Air classifier underflow (reject) stream flowrate (t/h)
F : Air classifier feed stream flowrate (t/h)
u : Air classifier underflow (reject) stream particle size distribution in weight retained %
f : Air classifier feed stream particle size distribution in weight retained %

Efficiency curve of the static air classifiers are compared in Figure 13. Performance parameters of the curves are tabulated in Table 6. d50 is the separation size which is defined as the size for which 50% of the particles in the feed report to underflow or reject stream (Wills and Napier Munn, 2008). By-pass represents the portion that reports to reject stream without classification. Fish-hook parameter characterizes the difference between the maximum percentage of fine material amount that appears in coarse stream and the bypass percentage as defined in Genç (2016). The slope of the curve expresses the efficiency of the classification and also known as imperfection (I) as defined in Wills and Napier Munn (2008). The slope can be calculated by Equation 3. As the slope of the curve increases, efficiency gets higher as stated in Wills and Napier Munn (2008). Static air classifier imperfection values are given in Table 6. Classification efficiency of the static air classifier in circuit-B got higher as compared to the one in circuit-A based on the calculated imperfection values.

Although mill discharge particle size distribution in circuit-B is finer than circuit-A as shown in Figure 11 coarser particle size distribution was obtained in static separator fine stream. Classification efficiency was also determined to be higher in circuit-B. In this context, coarser final product particle size distribution in circuit-B could be related to the lower circulating load as less amount of coarser particles

were rejected to the mill for further grinding. In that case, air classifier cut size was increased and coarser final product was obtained. Thus, operational conditions such as air flowrate, adjustable guide vane positions through which the material-laden air enters the inner cone of the separator and by adjusting the top outlet duct as stated in Genç (2008) could be optimized. For example; the cut-size can be varied by vertical adjustment of the air outlet duct at the top of the separator. For a constant air flowrate, an increase in length of this duct will within limits shift the cut size so as to give a finer product and vice versa as stated in Kohlhaas (1983). Another reason for obtaining much coarser particle size distribution in static air classifier fine stream could be the operational air classifier feed rate which was increased in circuit-B.

$$I = \frac{d_{75} - d_{25}}{2d_{50}} \quad (3)$$

d_{75} : particle size at which 75% of the feed particles report to reject stream (μm)
d_{25} : particle size at which 25% of the feed particles report to reject stream (μm)
d_{50} : particle size at which 50% of the feed particles report to reject stream (μm)

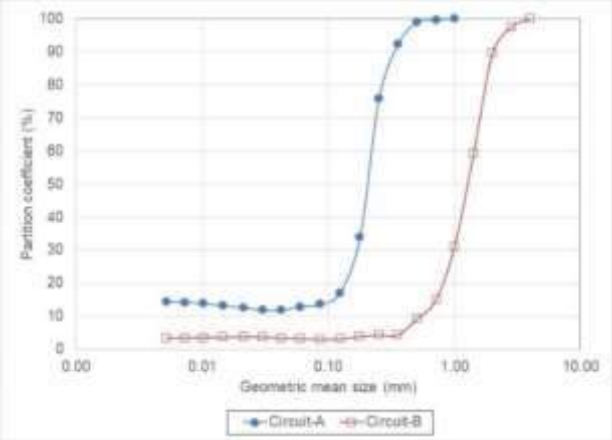

Figure 13. Efficiency curves of static air classifiers in circuit-A and circuit-B

Table 6. Efficiency curve and operational parameters

Parameters	Circuit-A	Circuit-B
d50 (mm)	0.21	1.26
By-pass (%)	11.84	3.00
Fish-hook (%)	2.55	1.41
Slope (m)	0.24	0.30

CONCLUSIONS

Size reduction performance of the single compartment air-swept ball mills and static air classifiers in cement raw material grinding circuits were evaluated. Findings indicated that, specific energy savings of 48.47% could be achieved with the operational conditions in circuit-B. Raw material mill feed particle size distribution fineness, grindability values were the important parameters in obtaining finer material from the mill. In this respect, optimization of blasting conditions in the open-pit mining stage, integration of pre-crushers as HPGRs and screens which will alter feed fineness and grindability of the material that is fed to the ball milling stage should be considered to increase the circuit capacity rates. On the otherhand, air classifier should also be operated at its optimum operational conditions which will effect the circulating loads in the circuit and cut size in obtaining finer final product from the grinding circuit.

ACKNOWLEDGEMENTS

Authors would like to acknowledge to the Turkish Scientific and Technical Research Council (Project no: 104M369) and the researchers involved for their valuable help.

REFERENCES

Austin, L.G., Klimpel, R.R., and Luckie, P.T. (1984). *Process Engineering of Size Reduction:* Ball Milling, A.I.M.E., S.M.E. New York, USA.

Duda, W.H. (1985). Cement-Data-Book, International Process Engineering in the Cement Industry, Vol.1, 3rd edition. 76-79pp.

Genç. Ö., 2016. Optimization of an industrial scale open circuit three-compartment cement grinding ball mill with the aid of simulation. International Journal of Mineral Processing. 154, pp.1-9.

Genç, Ö. (2008). An investigation on the effect of design and operational parameters on grinding performance of multi-compartment ball mills used in the cement industry. PhD Thesis. Hacettepe University, Mining Engineering Department, Turkey (In English).

Ghosh, S.N. (1991). Cement and Concrete Science & Technology, Volume I, Part I. First Edition. pp59.

JKSimMet Software V4.32, 1998, JK Tech, SMI, The University of Queensland, Brisbane, Australia.

Kohlhaas, B. (1983). Cement Engineers' Handbook, Fourth English Edition.

Napier-Munn, T.J., Morrell, S., Morrison, R.D., Kojovic, T. (2005). Mineral comminution circuits their operation and optimization. JKMRC Monograph Series in Mining and Mineral Processing, No.2 The University of Queensland, Brisbane, Australia.

Wills, B.A., Napier-Munn, T.J. (2008). Will's Mineral Processing Technology. pp214.